CrossMark

Surface morphology and crystal orientation of electrodeposited tungsten coatings with different pulse parameters

Xian-Qin Fang, Ying Zhang* , **Kai-Gui Zhu, Wen-Jia Han, Jian-Gang Yu, Zhe Chen, Hui-Jun Shi**

Abstract This study was conducted to investigate the influence of pulse parameters on the surface morphology and crystal orientation of the tungsten coatings electrodeposited on pure copper substrates. The deposited coatings were analyzed by X-ray diffraction (XRD), scanning electron microscopy (SEM) and energy-dispersive spectrometer (EDS). SEM analysis indicates that pulse parameters have significant influences on the surface morphology of the deposited coatings. Meanwhile, the change in grain size of the tungsten coatings demonstrates that the change in frequency and duty cycle could cause the variation of nucleation rate and grain growth of deposits. Moreover, no obvious diffusion layer at the coating/substrate interface is found by line analysis of EDS. XRD results reveal that tungsten coatings are of bcc structure and the preferred orientation of the deposits varies with duty cycle and period.

Keywords Tungsten coating; Electrodeposition; Pulse parameters; Crystal orientation; Surface morphology

1 Introduction

Nuclear fusion is considered to be the ideal source of environmentally friendly energy for the future due to its inherent safety, cheapness, abundant fuel and minimum radioactive waste [1, 2]. At present, the largest project of

X.-Q. Fang, Y. Zhang*, K.-G. Zhu, W.-J. Han, J.-G. Yu, Z. Chen, H.-J. Shi
Beijing Key Laboratory of Advanced Nuclear Energy Materials and Physics, School of Physics and Nuclear Energy Engineering, Beihang University, Beijing 100191, China
e-mail: zhyi@buaa.edu.cn

nuclear fusion is the International Thermonuclear Experimental Reactor (ITER), which has reached a high level of development in all major fusion programs [3]. However, the plasma-facing materials have to meet very complex requirements during fusion power reactor operation. Nowadays, high Z material is considered as the potential plasma-facing material (PFM) [4]. Tungsten has the highest melting point (3683 K), the lowest vapor pressure (1.3×10^{-7} Pa at melting temperature) and good erosion resistance. Furthermore, owing to high-energy threshold for physical sputtering under hydrogen bombardment and low tritium retention, tungsten seems to be a promising high Z material for PFM in fusion experimental devices [5–7]. Nonetheless, considering the high hardness and brittleness, tungsten is very difficult to process. A solution to overcome some of these problems is to deposit tungsten coating on some based materials [8]. At present, tungsten coatings were deposited by some techniques including magnetron sputtering [9], vacuum plasma spray [10], chemical vapor deposition [11] and physical vapor deposition [12], which have been widely applied to other materials [13–15]. Compared with these methods, many researchers have paid close attention to pulse electrodeposition. Microstructure and morphology of deposited tungsten can be controlled effectively by varying pulse frequency (f), current-on time (t_{on}), current-off time (t_{off}), peak current density (I_p), average current density (I_a) and duty cycle (γ) [16]. Some important relationships of these variables are given as below [17]:

$$\gamma = \frac{t_{on}}{t_{on} + t_{off}} \times 100\% \tag{1}$$

$$f = \frac{1}{t_{on} + t_{off}} \tag{2}$$

$$I_a = I_p \times \gamma \tag{3}$$

In addition, as far back as 1956, Davis and Gentry [18] had already reported that electrodeposition of tungsten coating is possible in $Li_2B_2O_4$–$Na_2B_2O_4$ ($K_2B_2O_4$)–WO_3 molten salt at 1173 K. And Nakajima et al. [19, 20] had succeeded in obtaining smooth and adhesive tungsten film from fluoride–chloride–WCl_4 (WO_3) molten salt at 523 K.

In this paper, in order to deposit compact and smooth tungsten coating on pure copper substrate, Na_2WO_4–WO_3 binary oxide molten salt was selected as electrolyte. Na_2WO_4–WO_3 melt is chemically stable, nonvolatile, non-hygroscopic, low cost and easily prepared [21]. The microstructure and composition of tungsten coatings were investigated firstly. Then, pulse parameters, such as duty cycle, period and frequency, were studied in detail, which have obvious influence on the surface morphology and crystal orientation of electrodeposited tungsten coatings.

2 Experimental

All the chemicals used in this experiment are of analytic pure reagents. Na_2WO_4 was dried in a furnace at 623 K for 24 h, and WO_3 was dried at 573 K for 8 h or longer. The anhydrous reagents were well mixed (mole ratio of Na_2WO_4 to WO_3 of 3:1) in an alumina crucible, and the eutectic Na_2WO_4–WO_3 composition was melted at the temperature of 1173 K in a vertical electric resistance furnace. The working electrode was a pure copper plate (99.6%, 20 mm × 10 mm × 5 mm), and a purity tungsten plate (99.9%, 20 mm × 10 mm × 5 mm) was taken as counter electrode. Prior to the deposition, the electrode's surface was mechanically polished to remove scratches, grease and oxide skin. After that, the samples were cleaned, respectively, in acetone and deionized water by ultrasonic cleaning for 5 min.

The two electrodes were set in eutectic salt in the furnace, and electrode distance kept 5 cm. And then, tungsten coating was prepared on pure copper substrate in atmosphere at a constant current density of 40 mA·cm^{-2}. After the process of electrodeposition, the obtained sample was immediately immersed into 5 mol·L^{-1} NaOH aqueous solution to wash away coherent salts and then cleaned by distilled water.

The phase composition and crystal orientation of tungsten coatings were determined by X-ray diffractometer (XRD, XRD-6000), operating with CuKα radiation at a scanning rate of 5 (°)·min^{-1} and 2θ scanning range of 10°–90°. The microstructure and surface morphology of deposits were analyzed by scanning electron microscopy (SEM, Quanta 250 FEG), and the cross-sectional morphology was measured by scanning electron microscopy

(SEM, JSM-7500F). Elemental analysis of the tungsten coatings was examined by energy-dispersive spectrometer (EDS, IE 300 X). File test was applied to evaluate the adherence of electrodeposited coating.

3 Results and discussion

### 3.1 Microstructure and composition of tungsten coatings

The metallic tungsten coatings were electrodeposited on pure copper substrates at the current density of 40 mA·cm^{-2} in atmosphere. Figure 1a shows the surface morphology of the sample electrodeposited for 2 h. The tungsten coating is compact and smooth without any cracks or voids. XRD pattern of the tungsten coating is shown in Fig. 1b. The scan data exhibit the strong diffraction 2θ peaks at 40.30°, 58.30°, 73.22° and 87.02°, respectively, corresponding to the (110), (200), (211) and (220) peaks. The result reveals that the tungsten coating consists of α-W phase that is bcc structure.

Figure 1c shows EDS analysis of tungsten coating. It can be observed that the deposit displays a strong peak of tungsten (W) and a reasonably weak peak of oxygen (O). The O detected in the deposit may result from the oxidation of W when the electrodeposition was over, because tungsten starts to oxidize in air from 873 K [22].
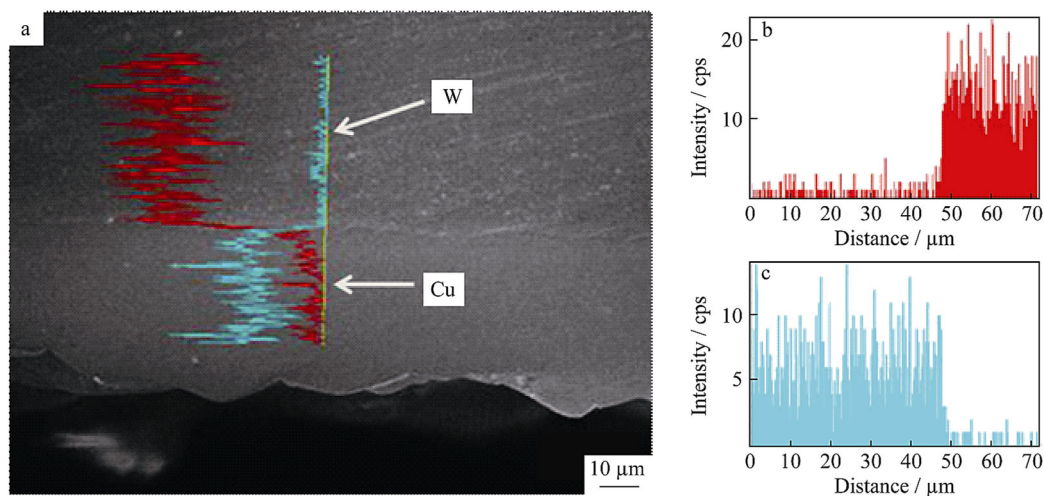
The line scanning curve and elemental distribution of the sample are shown in Fig. 2, also showing cross-sectional morphology of the coating. It can be seen that no observable voids, micro-cracks and other defects exist on the coating and interface surfaces. In addition, the tungsten coating is not separated from the substrate by file test. It is demonstrated that the tungsten coating exhibits excellent adherence with the substrate. Moreover, according to the line EDS analysis, no obvious diffusion layer between the tungsten coating and the copper substrate is found. There are two factors accounting for this phenomenon: (1) tungsten has an bcc structure, while the copper matrix possesses a fcc structure [23]; (2) the atomic radius between the two elements (tungstic atomic radius of 0.137 nm, copper atomic radius of 0.128 nm.) is different in the same coordination number (CN = 12) [24]. Therefore, the coating/substrate interface could scarcely mutually diffuse during electrodeposition.

3.2 Pulse parameters influence on surface morphology of deposited coatings

The deposition of metallic coatings by pulse electrodeposition depends on two fundamental processes, which are nucleation and growth of grains [25]. These two processes
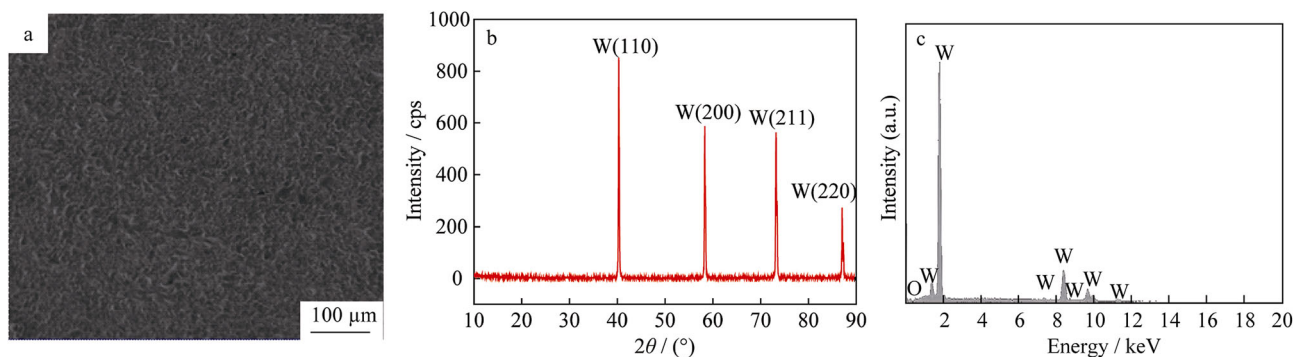
Fig. 1 SEM image of surface morphology **a**, XRD pattern **b** and EDS analysis **c** of tungsten coating deposited on copper substrate


Fig. 2 SEM image for line scanning analysis **a** and elemental distribution of sample: **b** Cu and **c** W

are contradictory in some pulse parameters of electrodeposition, such as pulse frequency and duty cycle.

Figure 3 shows SEM images of tungsten coatings' surface obtained at current density of 40 mA·cm^{-2} and duty cycle of 30% with various pulse frequencies. It is obviously observed that the grain size of tungsten coatings decreases with pulse frequency increasing from 100 to 250 Hz and then increases with the frequency increasing from 250 to 1000 Hz,. This result indicates that frequency is attributed to the formation of grains. Moreover, there is an appropriate value of pulse frequency that is conducive to grain refinement when the frequency changes. The pulse frequency of electrodeposition is not a fundamental parameter for grain size control at higher I_{p} (higher than 1 A·cm^{-2}), while both t_{on} and t_{off} influence the electrocrystallization process effectively [25–27].
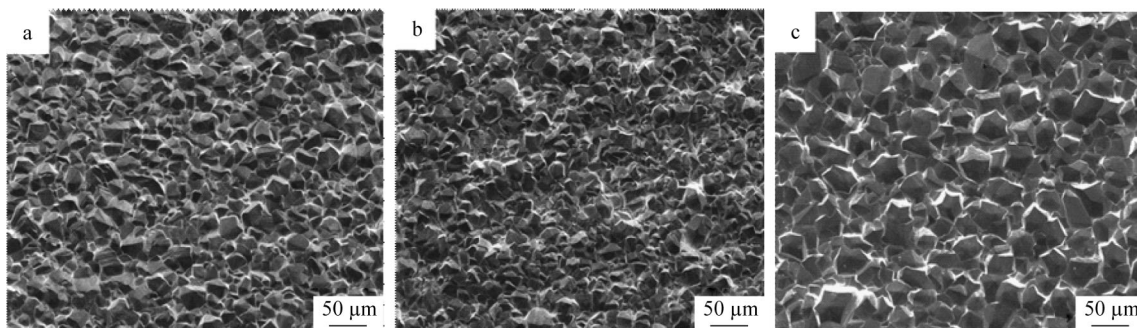
Fig. 3 Surface SEM images of tungsten coatings on copper substrates at different pulse frequencies: **a** 100 Hz, **b** 250 Hz, and **c** 1000 Hz

During pulse electrodeposition, duty cycle is a crucial parameter, because the properties of deposits can be influenced by both current-on time during which the formation of nuclei and growth of exiting crystal occur and current-off time during which deposition of ions takes place [28]. Here, tungsten coatings were prepared at duty cycles of 10, 30, 50 and 70% with $I_a = 40$ mA·cm^{-2} and $f = 1000$ Hz. The surface morphologies of tungsten coatings are presented in Fig. 4. As can be seen, the grain size of tungsten coatings is smaller at duty cycle of 10% than that at duty cycle of 30%. What can be explained for the result is that the crystals do not have sufficient time to grow at the duty cycle of 10% [26]. By increasing the duty cycle from 30% to 70%, the nucleation rate of tungsten coating starts to increase, leading to the decrease in the grain size [29]. Based on the above analysis, it can be concluded that duty cycle is a function of the tungsten coatings' grain size.

3.3 Pulse parameters influence on crystal orientation of deposited tungsten coatings

The texture coefficient (TC) is used to describe the preferred crystal orientation of the deposits during electrodeposition at different conditions, which can be calculated by the following formula [27]:

$$TC = \frac{I_{hkl}/I_{hkl}^0}{(1/n)\sum (I_{hkl}/I_{hkl}^0)} \tag{4}$$

where I_{hkl} and I_{hkl}^0 are the diffraction intensity of the crystal plane (hkl) in the deposited and standard samples, respectively, and n is the number of reflection faces in the diffraction pattern. If the texture coefficient is greater than 1.0, it indicates the existence of a preferred orientation.

The calculated results of tungsten coatings on the preferred orientation at different electrodeposited durations are illustrated in Fig. 5. It is evidently noticed that (200) intensity is the strongest of all samples at different durations, especially at 2 h. The (211) intensity decreases firstly and then increases; for the orientations of (110) and (220), their intensities are relatively weak. Therefore, it can be observed that the preferred orientations of the deposits are influenced slightly by electrodeposited duration.

From the calculation, the crystal orientations of deposits at different pulse periods are plotted in Fig. 6. It is indicated that the preferred orientation of tungsten coatings changes with the variation of pulse periods. As regards (200) orientation, it possesses the strongest intensity at the period of 1 ms. However, the texture coefficient of (200) decreases to 1.481 when the period is up to 4 ms, but (200) is still the preferred orientation. When the period reaches
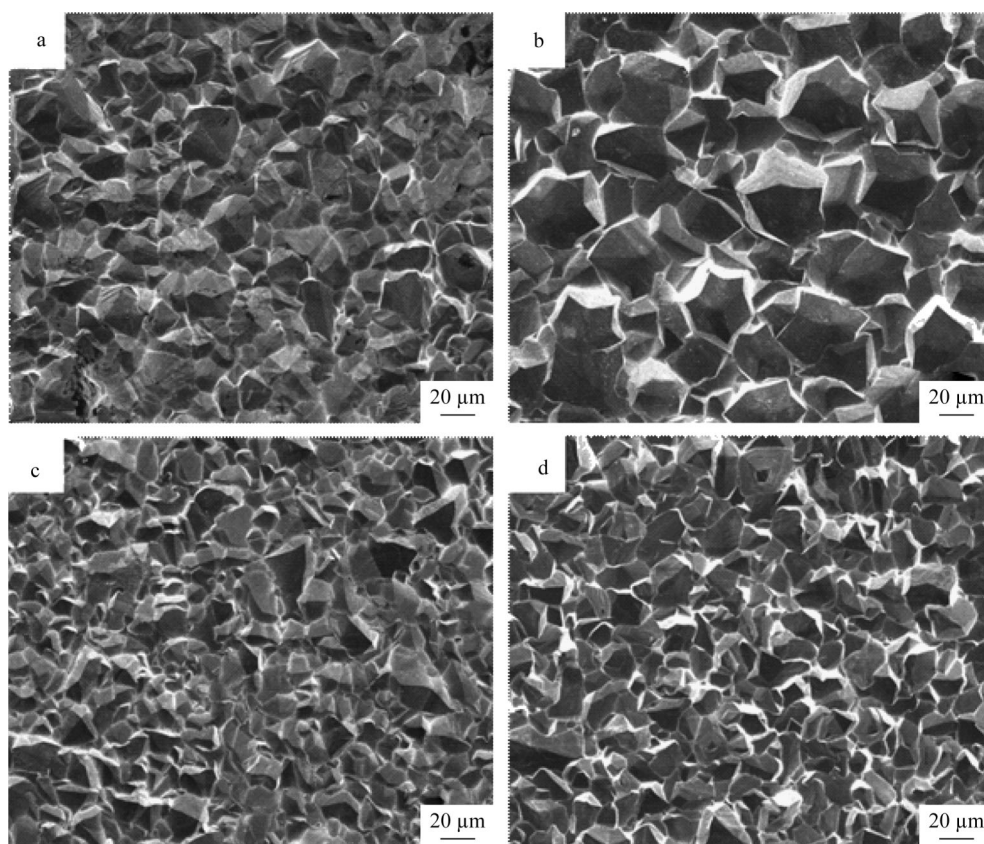

Fig. 4 Surface SEM images of tungsten coatings on copper substrates at different duty cycles: **a** 10%, **b** 30%, **c** 50% and **d** 70%
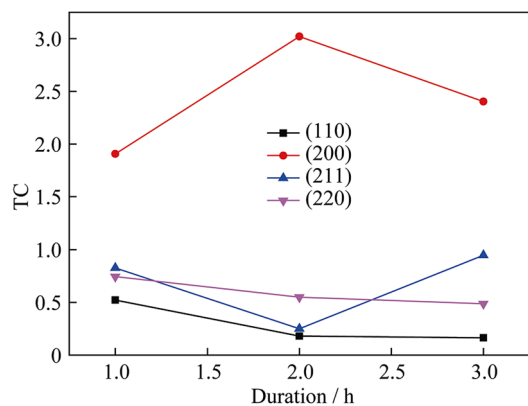
Fig. 5 Texture coefficient of tungsten coatings at different electrodeposited durations for duty cycle of 30% and period of 1 ms
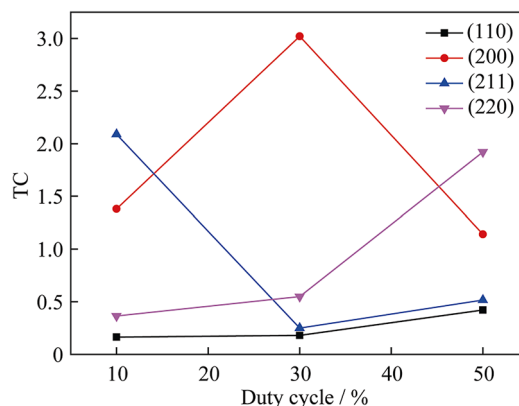
Fig. 7 Texture coefficient of tungsten coating at different duty cycles for electrodeposited durations of 2 h and period of 1 ms
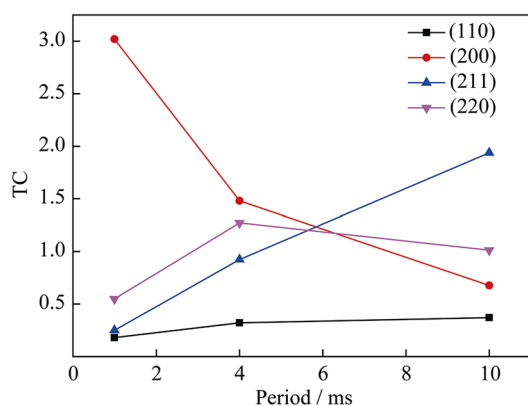
Fig. 6 Texture coefficient of tungsten coatings at different periods for duty cycle of 30% and electrodeposited durations of 2 h

The experimental results indicate that pulse parameters have pronounced influences on the crystal orientation of deposits. However, since varying current-on time (t_{on}) is known to affect period and duty cycle, the observed transition in crystal orientation may be attributed to the effect of increased t_{on}: (1) the depletion of cations at the cathode film, (2) the thickness of the pulsating diffusion layers, (3) the overpotential and (4) other absorption processes [30]. With respect to influence mechanism of these variables about transition in the crystal orientation, it is difficult to reveal clearly.

4 Conclusion

The obtained experimental results show that pure tungsten coatings deposited on the copper substrates from the Na_2WO_4–WO_3 binary oxide molten salt are compact and smooth without any cracks or voids. XRD results exhibit that tungsten coatings are of bcc structure. In addition, no obvious diffusion layer between tungsten coating and copper substrate is found by line analysis of EDS. Pulse parameters have great influences on surface morphology and crystal orientation of electrodeposited tungsten coatings. It is observed that the grain size of the tungsten coatings decreases firstly and then increases with the frequency increasing. The grain size and (200) intensity of the deposits exhibit a maximum value at 30% duty cycle. Furthermore, the preferred crystal orientation of the deposits changes from (200) to (211) or (220) with the period and duty cycle increasing.

10 ms, the preferred orientation changes from (200) to (211). In contrary to (200) intensity, the (211) intensity increases with pulse period increasing. And yet, by increasing the period, the (220) intensity increases at first and then decreases slightly; the (110) orientation varies smoothly with the change in period and its reflection is relatively weak.

As shown in Fig. 7, it is noted that the weakest crystal orientation is (110) at different duty cycles. As shown in Fig. 7, the variation of duty cycle could result in severe changes of (200), (211) and (220) reflections in the preferred orientation. The texture coefficient of (200) crystal orientation exhibits a peak value at duty cycle of 30%, and its intensities at duty cycles of 10% and 50% are 1.38 and 1.14, respectively. The tungsten coating exhibits a preferred (211) crystal orientation at duty cycle of 10%, but when duty cycle is up to 30%, the (211) intensity decreases so sharply that it is near to the lowest level and then starts to increase slightly. For (220) orientation, its intensity increases with the duty cycle increasing, and the strongest intensity at duty cycle of 50% reaches 1.92.

References

[[1] Matějíček J, Chraska P, Linke J. Thermal spray coatings for fusion applications—review. Therm Spray Technol. 2007; 16(1):64.

[2] Ongena J, Van Oost G. Energy for future centuries: will fusion be an inexhaustible, safe, and clean energy source? Fusion Sci Technol. 2004;45(2T):3.

[3] Rebut PH. ITER: the first experimental fusion reactor. Fusion Eng Des. 1995;30(1):85.

[4] Bolt H, Barabash V, Krauss W, Linke J, Neu R, Suzuki S, Yoshida N. Materials for the plasma-facing components of fusion reactors. In: Proceedings of the 11th International Conference on Fusion Reactor Materials. Kyoto; 2004. 66.

[5] Smid I, Akiba M, Vieider G, Plöchl L. Development of tungsten armor and bonding to copper for plasma-interactive components. In: Proceedings of the 8th International Conference on Fusion Reactor Materials. Sendia; 1998. 160.

[6] Davis JW, Barabash VR, Makhankov A, Plöchl L, Slattery KT. Assessment of tungsten for use in the ITER plasma facing components. In: Proceedings of the 8th International Conference on Fusion Reactor Materials. Sendia; 1998. 308.

[7] Tokunaga K, Yoshida N, Noda N, Sogabe T, Kato T. High heat load properties of tungsten coated carbon materials. In: Proceedings of the 8th International Conference on Fusion Reactor Materials. Sendia; 1998. 998.

[8] Ruset C, Grigore E, Maier H, Neu R, Greuner H, Mayer M, Matthews G. Development of W coatings for fusion applications. Fusion Eng Des. 2011;86(9):1677.

[9] Maier H, Luthin J, Balden M, Linke J, Koch F, Bolt H. Properties of tungsten coatings deposited onto fine grain graphite by different methods. In: Proceedings of the 7th International Conference on Plasma Surface Engineering. Partenkirchen; 2001. 733.

[10] Niu YR, Zheng XB, Ji H, Qi J, Ding CX, Chen JL, Luo GN. Microstructure and thermal property of tungsten coatings prepared by vacuum plasma spraying technology. Fusion Eng Des. 2010;85(7):1521.

[11] Du JH, Li ZX, Liu GJ, Qi HJ, Ding CX, Chen JL, Luo GN. Surface characterization of CVD tungsten coating on molybdenum substrate. Surf Coat Technol. 2005;198(1):169.

[12] Ganne T, Crépin J, Serror S, Zaoui A. Cracking behaviour of PVD tungsten coatings deposited on steel substrates. Acta Mater. 2002;50(16):4149.

[13] Chen A, Zhu K, Zhong H, Shao Q, Ge G. A new investigation of oxygen flow influence on ITO thin films by magnetron sputtering. Sol Energy Mater Sol C. 2014;120(A):157.

[14] Moon YT, Xie J, Liu C, Fu Y, Ni X, Biyikli N, Zhu K, Yun F, Sagar A, Feenstra RM. A study of the morphology of GaN seed on in situ deposited SixNy and its effect on properties of overgrowth of GaN epilayers. J Cryst Growth. 2006;291(1):301.

[15] Kuryatkov V, Zhu K, Borisov B, Chandolu A, Gherasoiu I, Kipshidze G, Chu SNG, Hotlz M, Kudryavtsev Y, Asomoza R, Nikishin SA, Temkin H. Electrical properties of p-n junctions based on superlattices of AlN/AlGa(In)N. Appl Phys Lett. 2003; 83(7):1319.

[16] Tao S, Li DY. Tribological, mechanical and electrochemical properties of nanocrystalline copper deposits produced by pulse electrodeposition. Nanotechnology. 2006;17(1):65.

[17] Chandrasekar MS, Pushpavanam M. Pulse and pulse reverse plating—conceptual, advantages and applications. Electrochim Acta. 2008;53(8):3313.

[18] Davis GL, Gentry CHR. The electrodeposition of tungsten. Metallurgia. 1956;53(1):3.

[19] Nakajima H, Nohira T, Hagiwara R. Electrodeposition of metallic tungsten in $ZnCl_2$–NaCl–KCl–WCl_4 melt at 250 °C. Electrochem Solid Sate Lett. 2005;8(7):C91.

[20] Nakajima H, Nohira T, Hagiwara R, Nitta K, Inazawa S, Okada K. Electrodeposition of metallic tungsten films in $ZnCl_2$-NaCl-KCl-KF-WO_3 melt at 250°C. Electrochim Acta. 2007;53(1):24.

[21] Jiang F, Zhang YC, Li XL, Sun NB, Wang LL. Tungsten coating prepared on V-4Cr-4Ti alloy substrate by electrodeposition from molten salt in air atmosphere. Fusion Eng Des. 2014;89(2):83.

[22] Lassner E, Schubert WD. Tungsten: Properties, Chemistry, Technology of the Element, Alloys, and Chemical Compounds. New York: Plenum Publishers; 1999. 85.

[23] Moseley PT, Seabrook CJ. The crystal structure of β-tantalum. Acta Crystallogr Sect B. 1973;29(5):1170.

[24] Hu GX, Cai X, Rong YH. Fundamentals of Materials Science. Shanghai: Shanghai Jiao Tong University Press; 2010. 5.

[25] Natter H, Hempelmann R. Nanocrystalline copper by pulsed electrodeposition: the effects of organic additives, bath temperature, and pH. J Phys Chem. 1996;100(50):19525.

[26] Moradi EH, Jafarzadeh K, Borji S, Abbaszadeh H. Pulse electrodeposition as a new approach in electrowinning of high purity cobalt from WC-Co scraps. Part I: the effect of frequency and duty cycle. Miner Eng. 2015;77:10.

[27] Kim SH, Sohn HJ, Joo YC, Kim YW, Yim TH, Lee HY, Kang T. Effect of saccharin addition on the microstructure of electrodeposited Fe–36 wt% Ni alloy. Surf Coat Technol. 2005; 199(1):43.

[28] Rajalakshmi N, Dhathathreyan KS. Nanostructured platinum catalyst layer prepared by pulsed electrodeposition for use in PEM fuel cells. Int J Hydrog Energy. 2008;33(20):5672.

[29] Liu YH, Zhang YC, Liu QZ, Li XL, Jiang F. The effects of electro-deposition current parameters on performance of tungsten coating. Int J Refract Met Hard Mater. 2012;35:241.

[30] Yuan XT, Wang Y, Sun DB, Yu HY. Influence of pulse parameters on the microstructure and microhardness of nickel electrodeposits. Surf Coat Technol. 2008;202(9):1895.